

# The Plasma Mantle: Polar Satellite Observations

20 December 1998

Prepared by

J. F. FENNELL and J. L. ROEDER  
Space and Environment Technology Center  
Technology Operations

M. GRANDE and C. PERRY  
Rutherford Appleton Laboratory  
Chilton, Didcot, Oxon, U.K.

R. FRIEDEL, A. KORTH, and B. L. VI  
Max-Planck-Institut für Aeronomie  
Katlenburg-Lindau, Germany

T. A. FRITZ  
Boston University  
Boston, MA

Prepared for

SPACE AND MISSILE SYSTEMS CENTER  
AIR FORCE MATERIEL COMMAND  
2430 E. El Segundo Boulevard  
Los Angeles Air Force Base, CA 90245

Engineering and Technology Group

This report was submitted by The Aerospace Corporation, El Segundo, CA 90245-4691, under Contract No. F04701-93-C-0094 with the Space and Missile Systems Center, 2430 E. El Segundo Blvd., Los Angeles Air Force Base, CA 90245. It was reviewed and approved for The Aerospace Corporation by A. B. Christensen, Principal Director, Space and Environment Technology Center. Michael Zambrana was the project officer for the Mission-Oriented Investigation and Experimentation (MOIE) program.

This report has been reviewed by the Public Affairs Office (PAS) and is releasable to the National Technical Information Service (NTIS). At NTIS, it will be available to the general public, including foreign nationals.

This technical report has been reviewed and is approved for publication. Publication of this report does not constitute Air Force approval of the report's findings or conclusions. It is published only for the exchange and stimulation of ideas.



\_\_\_\_\_  
Michael Zambrana  
SMC/AXE

# REPORT DOCUMENTATION PAGE

*Form Approved  
OMB No. 0704-0188*

Public reporting burden for this collection of information is estimated to average 1 hour per response, including the time for reviewing instructions, searching existing data sources, gathering and maintaining the data needed, and completing and reviewing the collection of information. Send comments regarding this burden estimate or any other aspect of this collection of information, including suggestions for reducing this burden to Washington Headquarters Services, Directorate for Information Operations and Reports, 1215 Jefferson Davis Highway, Suite 1204, Arlington, VA 22202-4302, and to the Office of Management and Budget, Paperwork Reduction Project (0704-0188), Washington, DC 20503.

1. AGENCY USE ONLY ( <i>Leave blank</i> )	2. REPORT DATE 20 December 1998	3. REPORT TYPE AND DATES COVERED	
4. TITLE AND SUBTITLE  The Plasma Mantle: Polar Satellite Observations		5. FUNDING NUMBERS  F04701-93-C-0094	
6. AUTHOR(S) J. F. Fennell, J. L. Roeder, M. Grande, C. Perry, R. Friedel, A. Korth, S. Livi, and T. A. Fritz			
7. PERFORMING ORGANIZATION NAME(S) AND ADDRESS(ES) The Aerospace Corporation Technology Operations El Segundo, CA 90245-4691		8. PERFORMING ORGANIZATION REPORT NUMBER  TR-99(8570)-10	
9. SPONSORING/MONITORING AGENCY NAME(S) AND ADDRESS(ES) Space and Missile Systems Center Air Force Materiel Command 2430 E. El Segundo Boulevard Los Angeles Air Force Base, CA 90245		10. SPONSORING/MONITORING AGENCY REPORT NUMBER  SMC-TR-00-40	
11. SUPPLEMENTARY NOTES			
12a. DISTRIBUTION/AVAILABILITY STATEMENT  Approved for public release; distribution unlimited		12b. DISTRIBUTION CODE	
13. ABSTRACT ( <i>Maximum 200 words</i> )  Since launch in February 1996, the Polar satellite has made numerous traversals of the high-latitude dayside magnetosphere. These traversals have covered the high-altitude regions of the low-latitude boundary layer, cusp, cleft, mantle, and polar cap. Often, as the Polar satellite traverses the high-latitude dayside magnetosphere, it leaves the soft precipitation region of the cusp or cleft and enters into the mantle plasma. There, the angular distribution of 1 to 10 keV ions changes character from a convecting near-isotropic one to convecting predominantly perpendicular ions that are weakly upflowing. Sometimes the predominantly perpendicular fluxes of ions are observed throughout the cusp, cleft, and mantle. These "trapped" ion signatures are relatively common, and the energy of the trapped ions is generally < 10 keV. The energy of the most poleward trapped population generally decreases with increasing latitude as is expected for the mantle plasma. The angular distributions of the downward-going < 10 keV ions have large "loss cones," indicative of a relatively weak mirror geometry in the magnetic field at high altitudes. The mantle ion fluxes observed on Polar show much the same flows, distributions, and spatial characteristics as those observed on HEOS [Rosenbauer <i>et al.</i> , 1975]. The composition of the ions at > 1 keV/q is predominantly solar wind as expected.			
14. SUBJECT TERMS  Polar satellite, Magnetosphere, Plasma mantle		15. NUMBER OF PAGES 7	
		16. PRICE CODE	
17. SECURITY CLASSIFICATION OF REPORT UNCLASSIFIED	18. SECURITY CLASSIFICATION OF THIS PAGE UNCLASSIFIED	19. SECURITY CLASSIFICATION OF ABSTRACT UNCLASSIFIED	20. LIMITATION OF ABSTRACT

## **Acknowledgments**

We would like to thank the many individuals at their respective institutions that made the Polar CAMMICE program a success. We especially thank W. Peterson of Lockheed for allowing us to use the TIMAS data and for helpful science discussions. The work performed at The Aerospace Corporation was supported partly by Air Force contract FP47P1-91PC-0089 and partly under subcontract GC 131165 to Boston University as part of the NASA grant NAG5-30368, which also supports the Boston University effort. The work at the Max-Planck-Institute for Aeronomy was supported by DARA contracts 50OC89131, 50OC95022, and 50OC89110.

## Contents

1.	Introduction.....	1
2.	Instrumentation .....	1
3.	Observations .....	2
3.1	May 15, 1997 mantle observations.....	2
3.2	May 14, 1997 mantle observations.....	5
3.3	Mixed cusp/mantle signatures.....	5
3.4	Mantle statistics.....	5
4.	Discussion.....	6
	References .....	6

## Figures

1.	Energy-time and pitch angle spectrograms of ions on May 15, 1997 for 0730–1130 UT .....	2
2.	Total ion energy flux distributions in velocity space for the four time intervals .....	2
3.	Line plots of the mantle ion angular distributions for ~0954 UT on May 15, 1997.....	3
4.	Phase space density perpendicular to the magnetic field near the noon-midnight meridian .....	3
5.	Like Fig. 1 but for May 14, 1997 .....	4
6.	HYDRA ion spectrogram for May 14, 1997 .....	4
7.	Occurrence of mantle observations with time of year as observed by MICS on Polar using $> 1$ keV/q ions .....	5
8.	Position of Polar/MICS mantle observations in Invariant Latitude and MLT.....	6

## 1. Introduction

The cusp is generally considered to be populated by magnetosheath plasma of solar wind origin, on open magnetic field lines. The low energy cusp ions are observed to extend poleward of the higher energy ions giving rise to an energy dispersion signature on standard energy-time spectrograms [Rosenbauer *et al.*, 1975; Reiff, *et al.*, 1977; Lockwood *et al.*, 1996]. This dispersion is a result of the ion time-of-flight effects on poleward convecting flux tubes. The low energy ions take longer to reach their mirror points from their high altitude entry point in the cusp than do the higher energy ions and thus they are convected further poleward during their transit. Thus, a satellite crossing from low to high latitudes through the cusp in the noon-midnight meridian observes a decrease with time (latitude) in the maximum energy of the ions. Separately, there may exist a relative magnetic intensity maximum along the particle's trajectory between its entry point and its mirror point. Such maxima may be sufficient to reflect a fraction of the upward moving component of the ion distribution back to lower altitudes, subsequently trapping some of the ions between two mirror points of a magnetic "bottle". For example, ions with a local pitch angle  $\sim 90^\circ$  at the Polar satellite altitudes may form a temporarily trapped population if a local field minimum exists at Polar alti-

tudes. A signature of such trapping would be the formation of ion pitch angle distributions with relatively large "loss cones" and peak flux intensities near  $90^\circ$  pitch angle. Such angular distributions can also form as a consequence of the reconnection process by which the ions are injected along cusp field lines that are also rapidly convecting poleward. The combination of a strong convection velocity and the initial field aligned earthward ion velocity converts, via the mirror force, to a nearly perpendicular ion flux at high polar latitudes with a poleward velocity component at Polar altitudes. These ions would also show a dominantly upward flow well poleward of the cusp/LLBL boundary (Lockwood *et al.* 1996). These signatures and the ion composition are used to identify the mantle population. In addition, we examined the low energy electron population which is not discussed here.

## 2. Instrumentation

For this study we used particle measurements from multiple instruments from the Polar satellite to look for the mantle ion signatures. Polar is in an approximately  $2 \times 9 R_E$  orbit at  $\sim 86^\circ$  inclination with an orbital period of  $\sim 18$  hours. We used data from the MICS (Magnetospheric Ion Composition Sensor) which measures ion fluxes in the energy range 1 - 400 keV/q and provides both ion mass and charge state identification [Wilken, *et al.*, 1990]. The

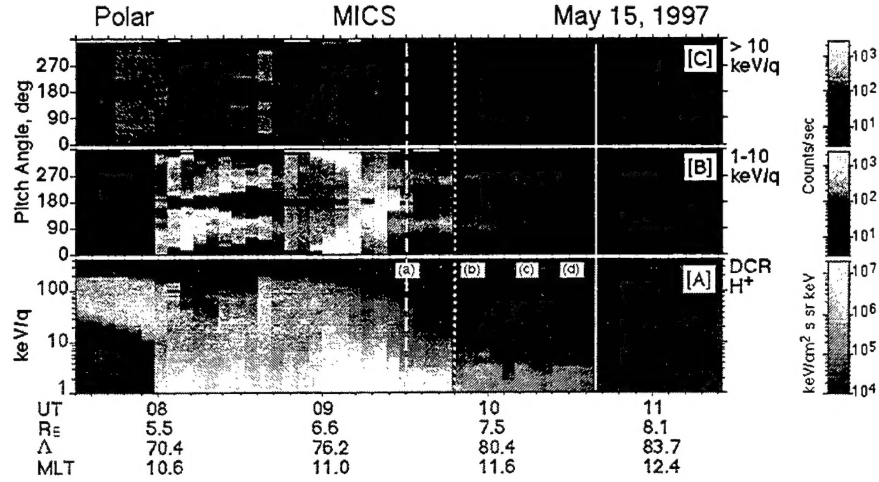


**Figure 1.** Energy-time and pitch angle spectrograms of ions on May 15, 1997 for 0730 - 1130 UT. Panel [A] shows the spin averaged energy-time spectrogram from the MICS total ion or DCR channel. Panel [B] shows the 1-10 keV/q ion intensity in each of 32 pitch angle bins for the data in panel [A]. Panel [C] shows the  $>10$  keV/q ion pitch angle distributions . The pitch angle coverage was not complete between 0806 UT and  $\sim$ 0850 UT, as is indicated by the dark patches in panels [B] and [C] near  $0^\circ$ ,  $180^\circ$ , and  $360^\circ$ . The vertical solid and dashed lines indicate the initial transition to mantle fluxes, a sudden change in the ion density and the transition from mantle to polar cap respectively (see text).

MICS sensor is mounted with its field of view perpendicular to the Polar spin axis. Its pitch angle coverage is complete only when the angle between  $B$  and the spin axis is  $90^\circ$ , otherwise MICS cannot view along the magnetic field direction. We used data from the TIMAS sensor [Shelley *et al.*, 1995], which covers essentially  $4\pi$  ster and measures the ion composition below 30 keV/q, to examine the relationship between the bulk plasma parameters and the MICS observations for one case. We also used data from the Hydra [Scudder *et al.*, 1995] plasma experiment to help identify the plasma regions.

### 3. Observations

The MICS composition measurements were used to identify the cusp by looking for intense high charge state ion fluxes corresponding to solar wind like charge states with emphases on the  $<10$  keV  $\text{He}^{++}$  and  $\text{O}^{2+}$  ions. Each cusp traversal was then examined for the existence of  $>1$  keV ions with the expected mantle signatures discussed above. The data examined covered the period from March 10, 1996 through May 1997. Mantle ion signatures were observed during  $\sim$ 70 traversals of the high latitude regions in the neighborhood and poleward of the cusp during this period. We present below two examples of cusp-mantle traversals from May 14-15, 1997 and provide some preliminary statistics on their occurrence in the Polar data set. All the observations that will be discussed were taken in the northern hemisphere at altitudes above  $\sim 5 R_E$ .

#### 3.1 May 15, 1997 mantle observations

The first example of a cusp and mantle traversal that occurred on May 15, 1997. is presented in Figure 1 in summary form. Fig. 1-[A] shows a total ion energy-time

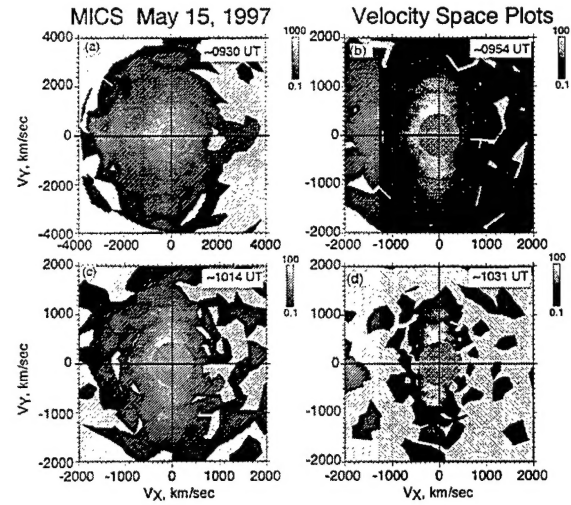


**Figure 2.** Total ion energy flux distributions in velocity space for the four time intervals 0930 (panel a), 0954 (panel b), 1014 (panel c) and 1031 UT (panel d) respectively for May 15, 1997. These correspond to the four markers (a), (b), (c) and (d) in Fig. 1.  $V_y$  is positive poleward perpendicular to  $B$  and  $V_x$  is positive earthward parallel to  $B$ .

spectrogram covering the energy range from 1-200 keV/q. It also shows that Polar was exiting the dayside plasma sheet near 10 MLT and entering the LLBL and cusp from 0755-0810 UT. Fig. 1-[B] and 1-[C] present the angular distributions for 1-10 keV/q and  $>10$  keV/q ions respectively. Fig. 1-[C] shows that MICS observed normal plasma sheet angular distributions with weak loss cones prior to 0800 UT. Between 0805 UT and 0855 UT the magnetic field was not perpendicular to the Polar spin axis and MICS did not obtain complete pitch angle coverage. After 0900 UT MICS did obtain complete angular distribu-

tions. What is clear in Fig. 1-[B] is that, as Polar traversed the poleward edge of the cusp and moved toward the polar cap, the 1-10 keV ion distributions were highly peaked almost perpendicular to the local magnetic field with a weaker secondary peak near 180° pitch angle. Between ~0950 and 1040 UT, there is little or no ion flux observed beyond  $90^\circ \pm 34^\circ$  (or  $270^\circ \pm 34^\circ$ ). Between 0830 UT and 0950 UT these highly peaked distributions appeared to "sit" on top of a nearly isotropic component. The maximum energy of the ions decreases (see Fig. 1-[A]) as Polar moved poleward and the 1-10 keV/q ion intensity decreased. Polar finally exited the plasma mantle near 1040 UT.

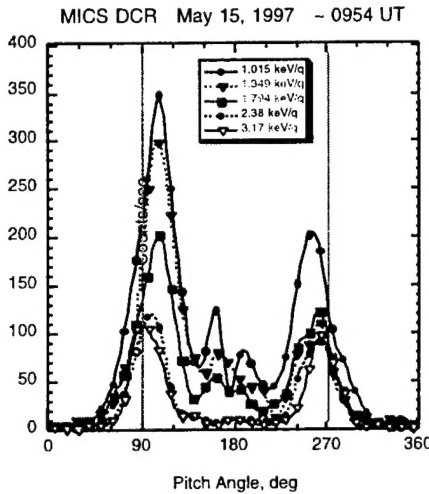


**Figure 3.** Line plots of the mantle ion angular distributions for ~0954 UT on May 15, 1997. These angular distributions were taken at point (b) in Fig. 1 and correspond to panel (b) in Fig. 2.

Each of the vertical lines in Fig. 1 corresponds to a significant change in the plasma, especially the angular distributions and density. For example, the Timas ion densities (not shown) exhibit dramatic drops near 0947 UT (primarily in the He ions and higher energy H<sup>+</sup>) and 1039 UT (all ions and energies). During this May 15, 1997 cusp/mantle crossing the cusp ion fluxes are very intense and very energetic. This event is one of the CEP (Cusp Energetic Particle) events discussed by Chen et al. (1997; 1998) and Chang et al. (1988). We will not discuss this aspect of the cusp/mantle traversal here and instead refer the reader to the referenced papers.

As noted above, the angular distributions of the 1-10 keV/q ions in Fig. 1-[B] appear to be highly constrained to pitch angles near 90° during the 0930 to 1040 UT interval. This is shown more clearly in Figure 2 which presents ion velocity space plots at four different times and Figure 3 where the ion pitch angle distributions, taken near 0954 UT, are plotted for several energies. The velocity space plots show the strong confinement of the ions to near  $V_x \sim 0$  as indicated by their broad extent in  $V_y$  but narrow extent in  $V_x$ . Initially there is a significant upflowing component of the >1 keV/q ion energy flux (see Fig. 2a) which slowly dies away (ref. Figs. 2b and 2c) until it is no

longer observable by 1020 UT (see Fig. 1-[B]). Fig. 2d shows what the velocity space distribution looked like after these upflowing field-aligned >1 keV/q ions disappeared.

Figure 3 shows detailed angular distributions of some of the ions from Fig 2b and makes obvious the fact that the bulk of the >1 keV/q ions are moving upward along the field lines and tailward. This is demonstrated by the fact that the intensity peaks in Fig. 3 are in the  $90^\circ$ - $270^\circ$  half plane where  $90^\circ$  corresponds to the poleward direction perpendicular to  $\mathbf{B}$ . The narrowness of the angular distribution after 0950 UT indicates that the mirror ratio, the ratio of the mirroring field intensity  $B_M$  to the local magnetic field intensity  $B$  for these particles with large pitch angles, is low ( $B_M/B \leq 1.5$ ).

The intensity difference between the ions with pitch angles near 105° and those near 255° is a consequence of the poleward convection (see Figure 4 below). Fig. 3 also clearly shows a relative peak in the angular distributions near 180° at the lowest energies. This upward going low energy field aligned component disappears more quickly with latitude than the near perpendicular component as shown in Figs. 1 and 2. The real curiosity is the fact that the relative peak near 180° exists. One would have expected the peak ion intensities near 105° and 255° to monotonically decrease towards 180°.

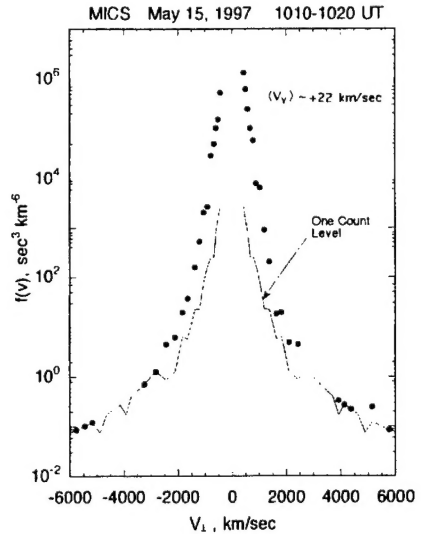


**Figure 4** Phase space density perpendicular to the magnetic field near the noon-midnight meridian. The average ion velocity derived from the data is ~ 22 km/sec poleward.

Figure 4 shows the total ion phase space density perpendicular to  $\mathbf{B}$  near 1015 UT (see Fig. 2c) for the >1 keV/q ions. The average drift velocity derived from this distribution is  $\langle V_y \rangle \sim +22$  km/sec, where + $V_y$  is tailward. This can be compared with a simultaneous estimate made using the <30 keV/q H<sup>+</sup> measurements from Timas (not shown) of  $\langle V_y \rangle \sim +24$  km/sec. This is very good agreement. Similarly, if the MICS data is used to estimate the average ion velocity parallel to the magnetic field one obtains  $\langle V_x \rangle \sim -300$  km/sec which seems much too high. The Timas estimate is  $\langle V_x \rangle \sim -30$  km/sec. The negative sign indicates the flow is anti-parallel to  $\mathbf{B}$ . The large value

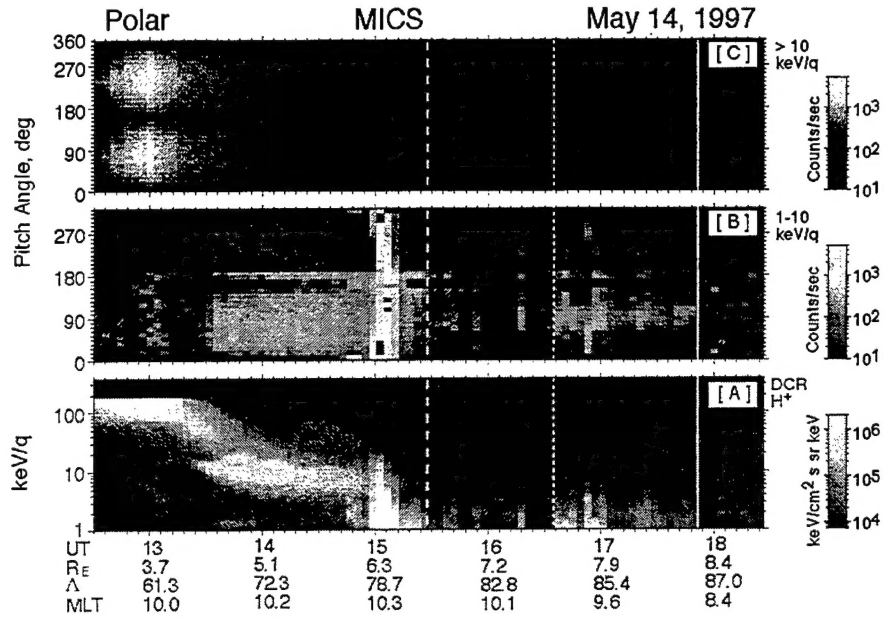


**Figure 5.** Like Fig. 1 but for May 14, 1997 (see text).

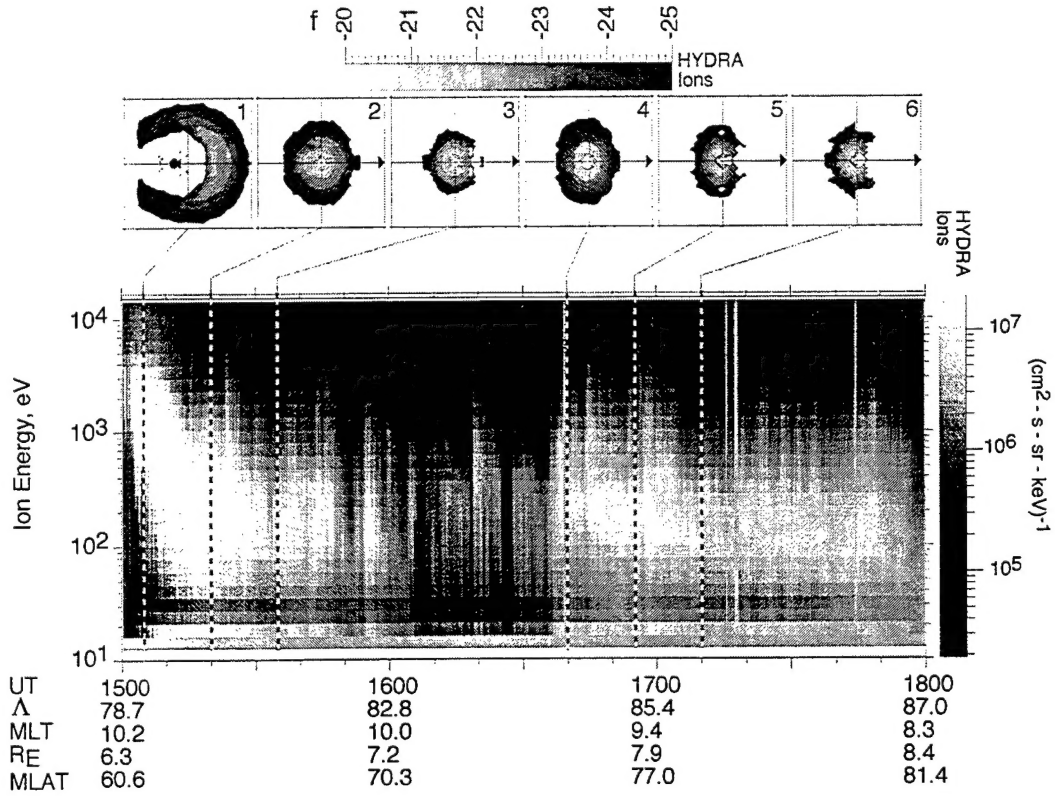


**Figure 6.** HYDRA ion spectrogram for May 14, 1997. The inset diagrams show the phase space density in velocity space with a velocity range of  $\pm 800$  km/sec.  $+V_x$  (parallel to  $B$ ) is indicated by the arrows.

of  $\langle V_x \rangle$  obtained from the MICS data results because the field aligned component of the MICS ion flux was at back-

ground while the anti-field aligned component was well above background. The lower energy coverage of Timas allows it to make a more accurate  $\langle V_x \rangle$  estimate.

### 3.2 May 14, 1997 mantle observations

Our second example of a cusp and mantle traversal was taken on May 14, 1997 and is summarized in Figure 5. The format of Fig. 5 is identical to that of Fig. 1. Here one sees that the cusp fluxes were observed in a narrow range of latitudes near 1500 UT. Fig. 5-[C] shows that all energetic ions ( $>10$  keV/q) disappeared at the low latitude edge of the cusp. Just prior to entering the cusp MICS observed bi-directional field aligned beams near 1449-1500 UT. The 1-10 keV/q ions in the cusp were flowing earthward near 1501-1506 UT. As Polar moved poleward of the cusp the angular distributions became generally upflowing starting near 1507 UT with little or no down-going flux near 1520 UT. The 1-10 keV/q ions were sporadic from 1530-1640 UT. From 1640-1755 UT mantle ion distributions were observed except for a short interval near 1658 UT where a burst of earthward flowing ions was observed. The earthward burst may have been a temporary recontact with cusp plasma. The mantle ion distributions were much like those observed on May 15, 1997 in Fig. 2c and 2d.

The Polar/Hydra instrument (Scudder *et al.*, 1995) observed the plasma ions during the whole period from 1500-1800 UT as shown in Figure 6. It is clear that what looked like a disconnected mantle region in Fig. 5 was an artifact of the MICS  $\sim 1$  keV/q energy threshold. The 1530-1640 UT region where MICS saw very little flux of 1-10 keV/q ions was a region of low intensity  $<1$  keV/q ions. The insets at the top of Fig. 6 are phase space density,  $f(v)$ , plots taken at the times indicated by the lines drawn to top of the spectrogram. The arrow to the right in each inset indicates the field line direction. Inset 1 shows  $f(v)$  in the cusp proper where the ions are flowing earthward parallel to  $B$ . Inset 3 shows the beginning of the upflowing mantle plasma. These upward flowing mantle ions are also shown in Insets 5 and 6 where there were essentially no ions in the  $+V_x$  direction. The MICS velocity space distributions (not shown) are entirely consistent with those from Hydra.

### 3.3 Mixed cusp/mantle signatures

There were cusp/cleft crossings wherein the ion angular distributions were much like those of Figs. 2 and 3 interspersed with cusp distributions much like those of Inset 1 in Fig. 6 throughout the traversal. One such example was published in a study of the May 29, 1996 magnetic cloud event by Grande *et al.* (1997). In that event (not shown) the  $>1$  keV/q ion angular distributions were much like those of Fig. 2d and Fig. 3 even at energies  $>20$  keV as observed by the CEPPAD IPS energetic proton measurements (ref. Fig. 4 of Grande *et al.*, 1997). During the May 29, 1996 event, as the magnetic field changed direction the ion angular distributions went back and forth from convecting nearly field aligned distributions like those of Inset 1 in Fig. 6 to convecting highly perpendicular distributions like those of Fig. 2d. During the May 29, 1996 event there was NOT a slow decrease in the maximum ion energy as the satellite moved poleward. This may have resulted because the solar wind pressure was high and variable and Polar was moving significantly in local time (from pre- to post-noon) during the crossing.

### 3.4 Mantle statistics

The seasonal dependence of the Polar mantle plasma observations by the MICS sensor are shown in Figure 7. Essentially mantle ions were not observed by MICS during the winter. Why is this? Basically, the Polar satellite was not in the appropriate position to observe the mantle plasma during the winter. The inset diagram at the top of Fig. 7 describes the orbital geometry. Polar is in a dawn-dusk orbit in the summer and winter periods and in the noon-midnight plane in the spring and fall. The combination of Polar's  $86^\circ$  inclination and the seasonal tilt angle of the geomagnetic dipole relative to the earth-sun line combines to put the polar satellite poleward of the mantle region during the winter but crossing the mantle region in spring through fall.

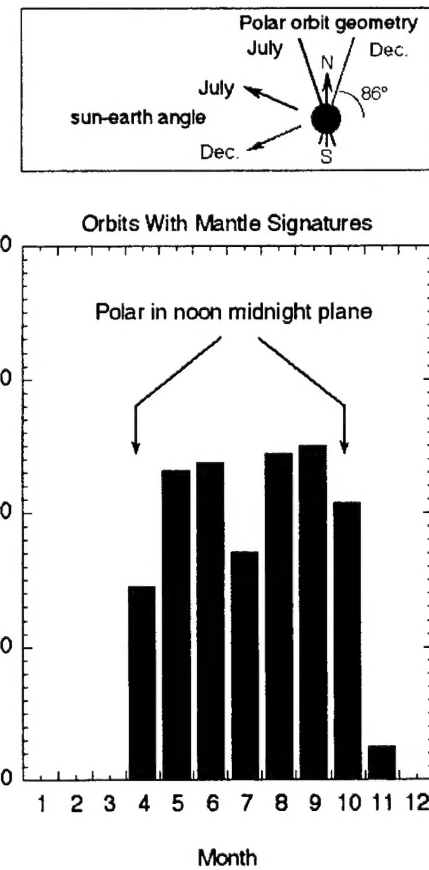
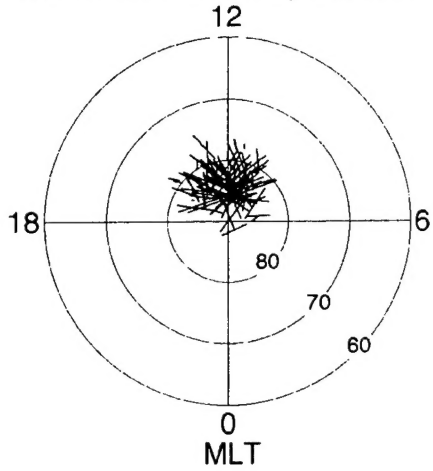


Figure 7. Occurrence of mantle observations with time of year as observed by MICS on Polar using  $> 1$  keV/q ions.

Figure 8 shows where mantle plasma was observed in MLT and Invariant Latitude. The individual line segments delineate the trajectory of the Polar spacecraft during the periods mantle ions were observed. The length of the lines reflects the duration and latitudinal-local time extent of the events. The majority of the mantle observations occurred for  $80^\circ < \Lambda < 87^\circ$  and they occurred within three hours of the noon-midnight meridian. This is generally consistent

with previous observations of the mantle (see discussion in Haerendel, and Paschmann, 1982, Newell *et al.*, 1991, and Sandahl *et al.*, 1997).

### Position of MICS Mantle Ion Observations March 10, 1996 - May 31, 1997



**Figure 8.** Position of Polar/MICS mantle observations in Invariant Latitude and MLT.

#### 4. Discussion

The examples we have shown differentiate the plasma mantle ions from the cusp or magnetosheath ions on the basis of their angular distributions and also on their composition (not shown). The mantle ions are the magnetically reflected cusp ions which flow anti-earthward while convecting tailward. The cusp ions were observed to have a dominantly earthward directed flow while they are being convected tailward. These two signatures are very different and allow easy distinction. All the mantle ion features observed by the Polar MICS experiment are consistent with those observed by the Hydra and Timas experiments on Polar. They are also generally consistent with the observations of the plasma mantle by low altitude (Newell *et al.*, 1991) and high altitude (Rosenbauer *et al.*, 1975; Sandahl *et al.*, 1997) satellites. As expected, these ions were observed near the poleward edge of the cusp and into the tail lobe and can persist at Polar for an hour or more.

We have shown the detailed velocity space distributions for only two cusp/mantle traversals. However, the MICS spectrograms from over 70 such events show the same general trends as seen in the MICS data on May 14,

and May 15, 1997. These features are, the nearly perpendicular to **B** ion fluxes that are upflowing and that are generally observed at the poleward portion of the cusp and more generally poleward of the cusp itself. The ions with these angular distribution signatures most often have an obviously lower density than do the cusp ions, as inferred from the observed ion intensities over the MICS energy range. The energy of the mantle ions rarely exceeds 10 keV, even during CEP (Chen *et al.*, 1997; 1998 and Chang *et al.*, 1998) events and are usually constrained to < 5 keV. In the future we will perform detailed examination of the composition aspects of the mantle ions.

**Acknowledgments.** We would like to thank the many individuals at their respective institutions that made the Polar CAMMICE program a success. We especially thank W. Peterson of Lockheed for allowing us to use the Timas data and for helpful science discussions. The work performed at The Aerospace Corporation was supported partly by Air Force contract FP47P1-91PC-0089 and partly under subcontract GC 131165 to Boston University as part of the NASA grant NAG5-30368 which also supports the Boston University effort.. The work at the Max-Planck-Institute for Aeronomy was supported by DARA contracts 50OC89131, 50OC95022, and 50OC89110.

#### References

- Chang, S.-W., et al., *Geophys. Res. Lett.*, in press, 1998.
- Chen, J., et al., *Geophys. Res. Lett.*, **24**, 1447-1450, 1997.
- Chen, J., et al., *J. Geophys. Res.*, **103**, 69, 1998.
- Grande, M., et al., *Geophys. Res. Lett.*, **24**, 1475-1478, 1997.
- Haerendel, G. and G. Paschmann, in *Magnetospheric Plasma Physics*, S. Nishida Ed., p. 49, Reidel, 1982
- Lockwood, M. S. et al., *J. Geophys. Res.*, **101**, 21501-21513, 1996.
- Newell, P. T., et al., *J. Geophys. Res.*, **96**, 35, 1991.
- Reiff, P. H., et al., *J. Geophys. Res.*, **82**, 479, 1977.
- Rosenbauer, H., et al., *J. Geophys. Res.*, **80**, 2723, 1975.
- Sandahl, I., et al., *Adv. Space Res.* **20**, 823, 1997.
- Shelley, E. G., et al., *Sp. Sci. Rev.*, **71**, 497-530, 1995.
- Scudder, J., et al., *Sp. Sci. Rev.*, **71**, 459, 1995
- Wilken, B., et al., *J. Spacecraft Rockets*, **29**, 585, 1992.

## **LABORATORY OPERATIONS**

The Aerospace Corporation functions as an "architect-engineer" for national security programs, specializing in advanced military space systems. The Corporation's Laboratory Operations supports the effective and timely development and operation of national security systems through scientific research and the application of advanced technology. Vital to the success of the Corporation is the technical staff's wide-ranging expertise and its ability to stay abreast of new technological developments and program support issues associated with rapidly evolving space systems. Contributing capabilities are provided by these individual organizations:

**Electronics and Photonics Laboratory:** Microelectronics, VLSI reliability, failure analysis, solid-state device physics, compound semiconductors, radiation effects, infrared and CCD detector devices, data storage and display technologies; lasers and electro-optics, solid state laser design, micro-optics, optical communications, and fiber optic sensors; atomic frequency standards, applied laser spectroscopy, laser chemistry, atmospheric propagation and beam control, LIDAR/LADAR remote sensing; solar cell and array testing and evaluation, battery electrochemistry, battery testing and evaluation.

**Space Materials Laboratory:** Evaluation and characterizations of new materials and processing techniques: metals, alloys, ceramics, polymers, thin films, and composites; development of advanced deposition processes; nondestructive evaluation, component failure analysis and reliability; structural mechanics, fracture mechanics, and stress corrosion; analysis and evaluation of materials at cryogenic and elevated temperatures; launch vehicle fluid mechanics, heat transfer and flight dynamics; aerothermodynamics; chemical and electric propulsion; environmental chemistry; combustion processes; space environment effects on materials, hardening and vulnerability assessment; contamination, thermal and structural control; lubrication and surface phenomena.

**Space Science Application Laboratory:** Magnetospheric, auroral and cosmic ray physics, wave-particle interactions, magnetospheric plasma waves; atmospheric and ionospheric physics, density and composition of the upper atmosphere, remote sensing using atmospheric radiation; solar physics, infrared astronomy, infrared signature analysis; infrared surveillance, imaging, remote sensing, and hyperspectral imaging; effects of solar activity, magnetic storms and nuclear explosions on the Earth's atmosphere, ionosphere and magnetosphere; effects of electromagnetic and particulate radiations on space systems; space instrumentation, design fabrication and test; environmental chemistry, trace detection; atmospheric chemical reactions, atmospheric optics, light scattering, state-specific chemical reactions and radiative signatures of missile plumes.

**Center for Microtechnology:** Microelectromechanical systems (MEMS) for space applications; assessment of microtechnology space applications; laser micromachining; laser-surface physical and chemical interactions; micropulsion; micro- and nanosatellite mission analysis; intelligent microinstruments for monitoring space and launch system environments.

**Office of Spectral Applications:** Multispectral and hyperspectral sensor development; data analysis and algorithm development; applications of multispectral and hyperspectral imagery to defense, civil space, commercial, and environmental missions.